

Band structure in ^{113}Sn

P. Banerjee,¹ S. Ganguly,² M. K. Pradhan,¹ H. P. Sharma,³ S. Muralithar,⁴ R. P. Singh,⁴ and R. K. Bhowmik⁴

¹*Saha Institute of Nuclear Physics, Sector-1, Block-AF, Bidhan Nagar, Kolkata-700064, India*

²*Department of Physics, Bethune College, Kolkata-700006, India*

³*Benaras Hindu University, Department of Physics, Varanasi-221005, India*

⁴*Inter University Accelerator Centre, New Delhi-110067, India*

(Received 27 April 2016; published 20 July 2016)

The structure of collective bands in ^{113}Sn , populated in the reaction $^{100}\text{Mo}(^{19}\text{F}, p5n)$ at a beam energy of 105 MeV, has been studied. A new positive-parity sequence of eight states extending up to 7764.9 keV and spin $(39/2^+)$ has been observed. The band is explained as arising from the coupling of the odd valence neutron in the $g_{7/2}$ or the $d_{5/2}$ orbital to the deformed 2p-2h proton configuration of the neighboring even- A Sn isotope. Lifetimes of six states up to an excitation energy of 9934.9 keV and spin $47/2^-$ belonging to a $\Delta I = 2$ intruder band have been measured for the first time, including an upper limit for the last state, from Doppler-shift-attenuation data. A moderate average quadrupole deformation $\beta_2 = 0.22 \pm 0.02$ is deduced from these results for the five states up to spin $43/2^-$. The transition quadrupole moments decrease with increase in rotational frequency, indicating a reduction of collectivity with spin, a feature common for terminating bands. The behavior of the kinematic and dynamic moments of inertia as a function of rotational frequency has been studied and total Routhian surface calculations have been performed in an attempt to obtain an insight into the nature of the states near termination.

DOI: [10.1103/PhysRevC.94.014316](https://doi.org/10.1103/PhysRevC.94.014316)

I. INTRODUCTION

Coexistence of both single-particle and collective structural features in nuclei near the proton shell closure at $Z = 50$ have been known for a long time and are reported in the literature [1,2]. We have reported detailed investigations of ^{111}In ($Z = 49$) [3], $^{111,112}\text{Sn}$ ($Z = 50$) [4,5], and ^{113}Sb ($Z = 51$) [6]. The low-energy states in these nuclei have been observed to be mostly spherical in nature, which is a manifestation of the proton shell closure at $Z = 50$. These spherical states have been interpreted to have a pure neutron configuration where the neutrons outside the $N = 50$ closed shell can occupy any of the positive-parity $s_{1/2}$, $d_{3/2}$, $d_{5/2}$, and $g_{7/2}$ and the unique-parity high- j $h_{11/2}$ orbitals. The neutron configuration changes as the neutron Fermi level increases with the neutron number N . The higher-energy states are based on the excitation of a pair of protons across the $Z = 50$ shell gap from the high- Ω , up-sloping $g_{9/2}$ orbital to the down-sloping low- Ω $g_{7/2}$ and $d_{5/2}$ orbitals leading to 2 particle-2 hole (2p-2h) type configurations. The down-sloping orbitals in the Nilsson diagram here are responsible for driving the nucleus to a prolate deformation and giving rise to deformed collective structures.

In the odd- A Sn isotopes, the collective bands arise from the coupling of the valence neutron, occupying different orbitals, to the deformed 2p-2h states of the neighboring even- A Sn nuclei. Several of these bands have been interpreted as smoothly terminating bands where the angular momentum is generated from the gradual alignment of the extra-core nucleons until all such nucleons are completely aligned and the band terminates in a noncollective oblate state at high spin. However, the experimental evidence in favor of such an interpretation is, so far, limited primarily to the observed gradual decrease of the dynamic moment of inertia $J^{(2)}$ with increasing spin to about a third of the rigid-body value. A more stringent test for band termination is the verification of the predicted decrease of collectivity as the band spin approaches

termination. Such verification exists only for ^{111}Sn [4], ^{109}Sb [7], and ^{113}Sb [6] where the transition quadrupole moments were found to decrease progressively with increase in spin.

Sears *et al.* [8] have reported three decoupled $\Delta I = 2$ rotational bands up to high spins in ^{113}Sn built upon the deformed 2p-2h proton configuration. The behavior of one of these bands was reported to be understood in the framework of smooth band termination. However, lifetime measurements were not reported in this work. Furthermore, the authors of Ref. [8] could not isolate a positive-parity band built on the $[20,4]$ configuration (using the shorthand notation of Ref. [9]; $[20,4]$ denotes two proton holes in the $g_{9/2}$ orbital, no proton in the $h_{11/2}$ orbital, and four neutrons in the $h_{11/2}$ orbital) although bands having $[21,4]^-$ and $[22,4]^+$ configurations (the positive and negative signs denote the $\alpha = +1/2$ and $-1/2$ signatures, respectively) have been observed in the two $N = 62$ nuclei ^{113}Sb [2,6] and ^{114}Te [10], respectively. The existence of the $[20,4]$ band in ^{113}Sn is predicted from theoretical calculations within the configuration-dependent shell-correction approach [8]. The present work is an attempt to study the lifetimes of the states belonging to the most strongly populated $\Delta I = 2$ rotational sequence, reported earlier [8], with the objective of providing a better insight into the structure of the band and to look for the possible existence of the predicted $[20,4]$ positive-parity band in ^{113}Sn .

II. EXPERIMENTAL METHOD

Excited states of ^{113}Sn were populated in the $^{100}\text{Mo}(^{19}\text{F}, p5n)$ reaction at a beam energy of $E = 105$ MeV at the 15UD Pelletron Accelerator at the Inter University Accelerator Centre (IUAC), New Delhi. The target consisted of isotopically enriched (99.5%) ^{100}Mo with a thickness of 2 mg/cm², evaporated on an 8 mg/cm² gold backing. About 2.5×10^{10} two- and higher-fold coincident events were

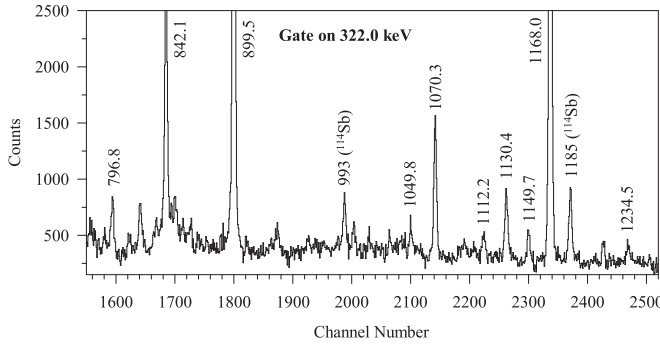


FIG. 2. Prompt γ -ray spectrum gated by the 322.0 keV γ ray. The $\Delta I = 2$ transitions belonging to band 2 and the 796.8 keV γ ray in band 4 (see text) are observed along with other γ rays.

other two $\Delta I = 2$ bands (labeled bands 1 and 2 in Ref. [8]) are observed to be weakly populated and are not included in the present study because significant new information could not be derived for these bands from the present data. Several states already reported earlier [8,15] are grouped into band 4 on the basis of the coincidence relationships between the γ rays depopulating the states. Gated spectra in support of the level scheme are shown in Figs. 2 and 3. Selected spectra at 90° and 148° with respect to the beam direction, along with the theoretical lineshape fits, are presented in Fig. 4. These spectra were used to determine the lifetimes of six states belonging to band 3. The results of the PDCO analyses are shown in Fig. 5. Figures 6, 7, 8, and 9 show plots for the experimental Routhians e' (for band 2), the transition quadrupole moments Q_t (for band 3), kinematic and dynamic moments of inertia $J^{(1)}$ and $J^{(2)}$ (for band 3), and the calculated total Routhian surfaces (TRSSs) (for band 3), respectively, and are discussed in Sec. IV. Tables I and II summarize the important experimental results obtained in the present work.

A. Bands 1 and 4

Band 1 is the negative-parity yrast sequence consisting of five states (Fig. 1) with the 739.0 keV, $11/2^-$ isomer as the bandhead. All five states have been previously reported [8,15]. The present R_{DCO} ratios (Table I) for the in-band transitions are consistent with the earlier spin and parity assignments for the states belonging to the band. The R_{DCO} ratios 0.87 ± 0.07 and 0.86 ± 0.08 for the 322.0 and 328.7 keV $\Delta I = 1$ transitions, respectively, in this sequence are in very good agreement with the previously reported results [8]. However, the multipole mixing ratios $\delta = 0.29 \pm 0.06$ and 0.28 ± 0.07 for the 322.0 and 328.7 keV γ rays (Table I) are somewhat larger than the corresponding results $\delta = 0.15 \pm 0.05$ and 0.16 ± 0.05 reported in Ref. [15]. The bandhead decays to a $7/2^+$, 78.0 keV isomer ($T_{1/2} = 21.4 \pm 0.4$ min) by the 661.0 keV $M2(+E3)$ transition [14,15].

The short sequence of five states built on the 1952.0 keV, $13/2^-$ state is labeled band 4 (Fig. 1). Several interband transitions connect bands 1 and 4. Four of the five levels in band 4 decay to states of band 1 while two states belonging to band 1 decay into states belonging to band 4. One of these is a new 57.7 keV transition and is proposed to connect the

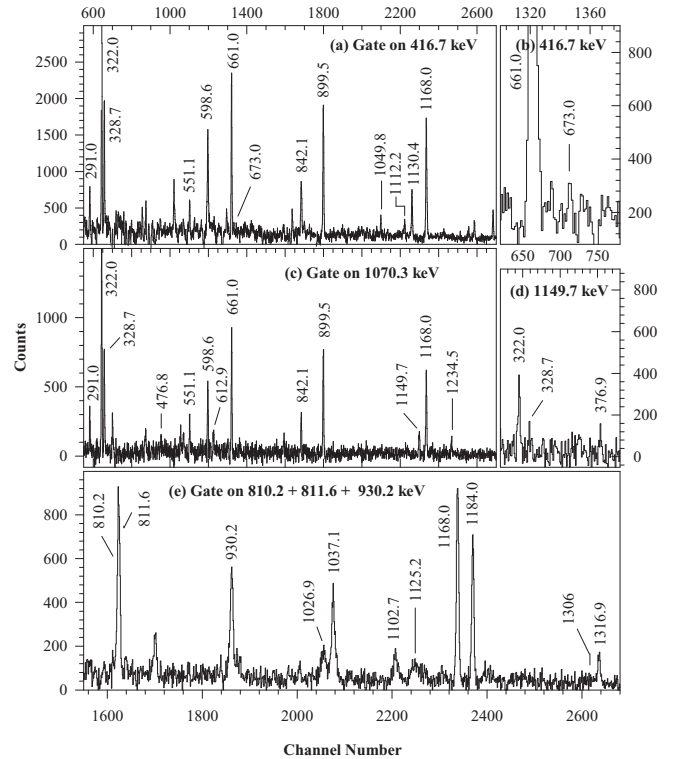


FIG. 3. Prompt γ -ray spectra gated by the (a), (b) 416.7, (c) 1070.3, and (d) 1149.7 keV transitions, belonging to band 2; spectrum (e) shows the sum of the spectra gated by the 810.2, 811.6, and 930.2 keV transitions, belonging to band 3. Only the 90° projection is shown in panel (e).

2806.5 (band 1) and 2748.8 keV (band 4) levels. This new placement is based on the observation of the strong 796.8 keV γ ray in the spectra gated by the 322.0 (Fig. 2) and 328.7 keV transitions. Direct evidence for the presence of the 57.7 keV γ ray in these gated spectra is weak due to the poor detection efficiency at low energies. In addition, a new 444.6 keV γ ray is tentatively proposed to connect the 3419.5 and 2974.9 keV states. The spectrum gated on the 551.1 keV transition gives a clear indication of the 444.6 keV γ ray. However, gates on the lower-lying transitions in band 4 could not render supportive evidence in favor of the placement.

Firm spin and parity assignments are adopted in the literature only for the two low-lying states at 1952.0 and 2748.8 keV in the sequence [14]. The I^π assignments for the three higher energy states are tentative in the literature. The present DCO measurements indicate that the 1067.9 keV interband transition has a stretched quadrupole character (Table I), suggesting a firm spin-parity assignment of $19/2^-$ for the 2974.9 keV state. Besides, the present R_{DCO} and the mixing ratios δ for the 291.0, 612.9, 551.1, and 842.1 keV γ rays (Table I) are consistent with firm I^π assignments of $21/2^-$ and $23/2^-$ for the 3419.5 and 3970.6 keV states, respectively. Hence, firm I^π assignments are proposed for all five states in band 4. It may be noted here that Sears *et al.* [8] made a tentative assignment of positive parity to the 3970.6 keV state. The 551.1 and 842.1 keV γ rays from this

TABLE I. Present experimental results on level energies (E_x), γ -ray energies (E_γ), γ -ray relative intensities, R_{DCO} , multipole mixing ratio δ , and spins of the initial and final states for transitions in ^{113}Sn based on the present work, unless indicated otherwise (see text).

Band	E_x (keV)	E_γ (keV)	Relative Intensity	R_{DCO}	Gating Transition (keV)	Multipolarity/ Mixing ratio δ	$J_i^\pi \rightarrow J_f^\pi$
1	739.0	661.0	> 100	0.93 ± 0.12	1168.0	$M2(+E3)^a$	$11/2^- \rightarrow 7/2^+$
	1907.0	1168.0	100 ± 8.4	0.99 ± 0.12	899.5	$E2$	$15/2^- \rightarrow 11/2^-$
	2806.5	57.7					$19/2_1^- \rightarrow 17/2_1^-$
		899.5	45.7 ± 4.1	1.12 ± 0.15	1168.0	$E2$	$19/2_1^- \rightarrow 15/2^-$
	3128.5	153.6	2.4 ± 0.5	0.69 ± 0.26	1168.0	$M1 + E2$	$21/2_1^- \rightarrow 19/2_2^-$
		322.0	39.5 ± 2.4	0.87 ± 0.07	899.5	0.29 ± 0.06	$21/2_1^- \rightarrow 19/2_1^-$
	3457.2	328.7	17.0 ± 1.3	0.86 ± 0.08	899.5	0.28 ± 0.07	$23/2_1^- \rightarrow 21/2_1^-$
4	1952.0	1213.0	4.7 ± 1.0			$M1 + E2^a$	$13/2^- \rightarrow 11/2^-^a$
	2748.8	796.8	4.1 ± 0.9			$E2^a$	$17/2_1^- \rightarrow 13/2^-^a$
	2974.9	226.1	2.2 ± 0.6			$M1 + E2$	$19/2_2^- \rightarrow 17/2_1^-$
		1067.9	6.0 ± 0.9	1.00 ± 0.19	1168.0	$E2$	$19/2_2^- \rightarrow 15/2^-$
	3419.5	291.0	4.3 ± 0.7	1.08 ± 0.25	899.5	$M1$	$21/2_2^- \rightarrow 21/2_1^-$
		444.6	~ 1				$21/2_2^- \rightarrow 19/2_2^-$
		612.9	2.4 ± 0.3	1.06 ± 0.16	899.5	$0.46^{+0.19}_{-0.14}$	$21/2_2^- \rightarrow 19/2_1^-$
	3970.6	551.1	6.4 ± 1.0	0.82 ± 0.16	1168.0	$0.25^{+0.13}_{-0.14}$	$23/2_3^- \rightarrow 21/2_2^-$
		842.1	11.6 ± 1.5	0.68 ± 0.11	899.5	$0.13^{+0.08}_{-0.10}$	$23/2_3^- \rightarrow 21/2_1^-$
	2	4055.8	85.2				$E1^a$
		598.6	14.2 ± 1.8	0.56 ± 0.09	899.5	$0.01^{+0.08}_{-0.09}$	$25/2^+ \rightarrow 23/2_1^-$
4472.5		416.7	12.7 ± 1.1	0.97 ± 0.11	899.5	$0.37^{+0.11}_{-0.10}$	$27/2^+ \rightarrow 25/2^+$
5126.1		1070.3	9.8 ± 1.2	1.03 ± 0.17	1168.0	$E2$	$29/2^+ \rightarrow 25/2^+$
5602.9		476.8	0.6 ± 0.2			$M1 + E2$	$31/2^+ \rightarrow 29/2^+$
		1130.4	5.0 ± 0.6	0.96 ± 0.15	899.5 + 1168.0	$E2$	$31/2^+ \rightarrow 27/2^+$
6275.8		673.0	0.6 ± 0.2			$M1 + E2$	$33/2^+ \rightarrow 31/2^+$
		1149.7	2.5 ± 0.5	0.96 ± 0.26	899.5 + 1168.0	$E2$	$33/2^+ \rightarrow 29/2^+$
6652.7		376.9	0.5 ± 0.2			$M1 + E2$	$35/2^+ \rightarrow 33/2^+$
		1049.8	1.6 ± 0.4	0.98 ± 0.30	899.5 + 1168.0	$E2$	$35/2^+ \rightarrow 31/2^+$
7510.3		1234.5	1.5 ± 0.3			($E2$)	$(37/2^+) \rightarrow 33/2^+$
7764.9		1112.2	1.3 ± 0.3			($E2$)	$(39/2^+) \rightarrow 35/2^+$
3	3901.2	677.2	8.1 ± 1.2	1.19 ± 0.24	1168.0	$E2$	$23/2_2^- \rightarrow 19/2_3^-$
		810.2	19.3 ± 3.7	1.13 ± 0.20	811.6	$E2$	$23/2_2^- \rightarrow 19/2_2^-$
	4712.8	811.6	24.6 ± 4.3	1.09 ± 0.23	810.2	$E2$	$27/2^- \rightarrow 23/2_2^-$
	5643.0	930.2	23.0 ± 3.3	1.13 ± 0.15	810.2 + 811.6	$E2$	$31/2^- \rightarrow 27/2^-$
	6680.1	1037.1	17.4 ± 4.1	0.96 ± 0.14	810.2 + 811.6	$E2$	$35/2^- \rightarrow 31/2^-$
	7782.8	1102.7	7.8 ± 1.3	1.06 ± 0.20	810.2 + 811.6	$E2$	$39/2^- \rightarrow 35/2^-$
	8809.7	1026.9	7.2 ± 1.8	1.04 ± 0.19	810.2 + 811.6	$E2$	$43/2^- \rightarrow 39/2^-$
	9934.9	1125.2	3.1 ± 1.7			$E2^b$	$47/2^- \rightarrow 43/2^-^b$
	11240.8	1306	~ 1			$E2^b$	$51/2^- \rightarrow 47/2^-^b$
	Other states	2851.5	899.5	3.4 ± 0.6			
		944.5	1.2 ± 0.4				$(17/2^-) \rightarrow 15/2^-^a$
3091.0		1184.0	21.1 ± 2.6	1.12 ± 0.20	1168.0	$E2$	$19/2_3^- \rightarrow 15/2^-$
3223.9		1316.9	9.7 ± 1.4	1.13 ± 0.19	1168.0	$E2$	$19/2_4^- \rightarrow 15/2^-$

^aFrom Ref. [14].

^bFrom Ref. [8].

state were both tentatively assigned to have a $E1$ character. Assuming this to be true, the present δ values for the two γ rays (Table I) are suggestive of too large a $M2$ component, especially for the 551.1 keV γ ray. Since such large $M2$ admixtures are usually not associated with $E1$ transitions, a negative parity has been proposed for the 3970.6 keV level in the present work. A tentative negative parity assignment is already adopted in the literature for the 3970.6 keV level [14] based on the results of Ref. [15].

B. Band 2

Band 2 is a new sequence built on the $25/2^+$, 4055.8 keV state as shown in Fig. 1. The eight new transitions in the band are indicated by asterisks in the figure. The band extends up to an excitation energy of 7764.9 keV and spin ($39/2^+$). All excited states, except those at 4472.5 and 5602.9 keV, have been observed for the first time. The latter state has so far been reported only by Sears *et al.* [8]. The band shows a small but significant amount of signature splitting with the $\alpha = -1/2$

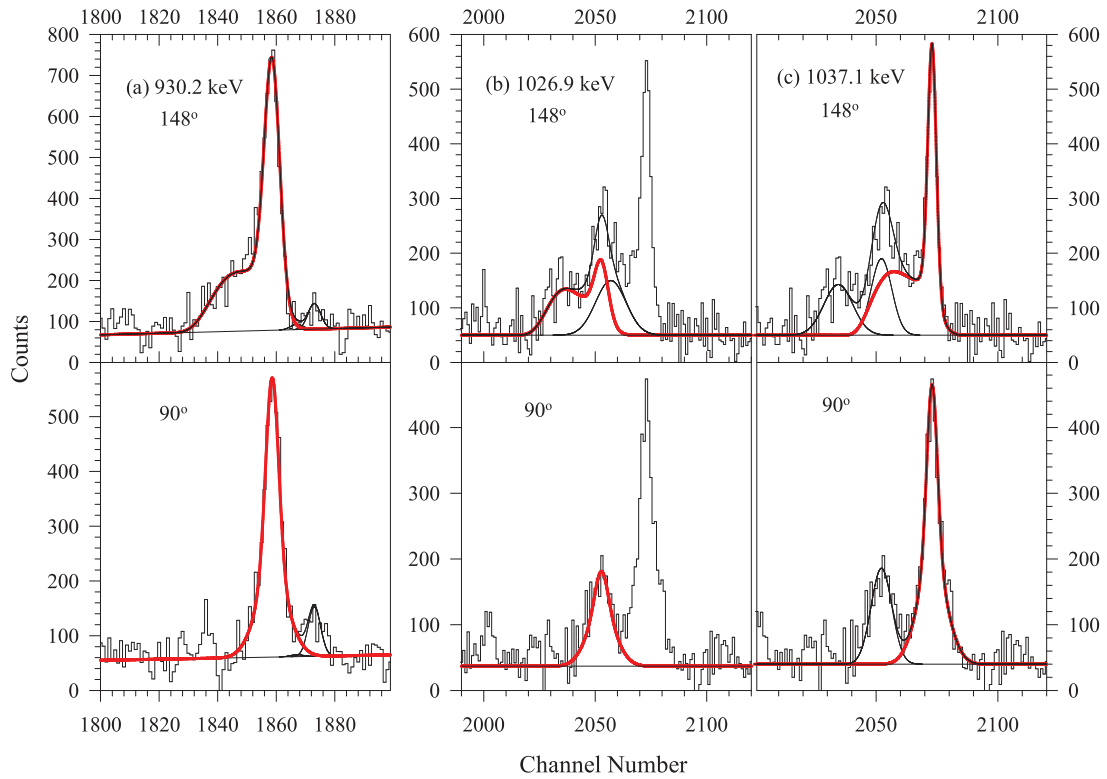


FIG. 4. Gated DSA spectra for (a) 930.2, (b) 1026.9, and (c) 1037.1 keV transitions belonging to band 3. The upper (lower) panel shows spectra projected at 148° (90°) with respect to the beam direction. Continuous lines are fits to the experimental data using the code LINESHAPE [12]. Details are given in the text.

signature partner being energetically favored (discussed in Sec. IV). Figure 2 shows the spectrum gated by the 322.0 keV γ ray. All six $\Delta I = 2$ transitions assigned to band 2 can be seen clearly in the spectrum in Fig. 2. However, the relatively weak $\Delta I = 1$ transitions are not observed in this spectrum. Spectra gated on the 416.7 keV γ ray and the new 1070.3 and 1149.7 keV γ rays are shown in Figs. 3(a)–3(d) in further support of the placement of the transitions in the band. The 1130.4, 1049.8, and 1112.2 keV transitions are observed in the spectrum gated by the 416.7 keV γ ray while the 1149.7 and the 1234.5 keV transitions are seen in the spectrum gated by the 1070.3 keV γ ray. The three relatively weak $\Delta I = 1$ transitions with energies 376.9, 476.8, and 673.0 keV are observed in the spectra gated by the 1149.7, 1070.3, and 416.7 keV transitions, respectively (see Fig. 3).

Firm spin and parity assignments have been made for all states in band 2 except the two highest observed states at 7510.3 and 7764.9 keV to which only a tentative assignment is possible. The spin-parity assignments have been done on the basis of the present DCO and polarization studies and the earlier results reported in Ref. [8]. Spin-parity assignments of $25/2^+$, $27/2^+$ and $31/2^+$ have previously been made for the bandhead at 4055.8 keV and the two excited states at 4472.5 and 5602.9 keV, respectively [8]. Spins of $25/2^+$ and $(27/2^+)$ were also proposed for the 4055.8 and 4472.5 keV levels by Käubler *et al.* [15]. The present DCO results (Table I) and the polarization studies, the results of which are shown in Fig. 5, corroborate these earlier assignments. The multipole mixing ratio $\delta = 0.01^{+0.08}_{-0.09}$ for the 598.5 keV γ ray is consistent with

its $E1$ assignment and a spin of $25/2^+$ for the 4055.8 keV state. The mixed $M1/E2$ and the stretched $E2$ character of the 416.7 and 1130.4 keV γ rays, respectively, proposed earlier [8], are also confirmed from the present DCO and PDCO results, lending support to the earlier spin assignments for the 4472.5 and 5602.9 keV states.

The R_{DCO} values for the new 1049.8, 1070.3, and 1149.7 keV γ rays, estimated from gating on $E2$ transitions, are all found to be close to unity (Table I), suggesting that the three γ rays are of the stretched quadrupole character. The PDCO results for the 1070.3 and 1149.7 keV γ rays, shown in Fig. 5, are consistent with an electric nature of the two transitions. Although a reliable PDCO measurement for the relatively weak 1049.8 keV γ ray was not possible, an $E2$ assignment for the γ ray appears to be consistent with its quadrupole character inferred from the R_{DCO} result and its placement in the band. Based on these results, firm spin and parity assignments of $29/2^+$, $33/2^+$, and $35/2^+$ are proposed for the 5126.1, 6275.8, and 6652.7 keV levels, respectively (Fig. 1). Measurements for the relatively weak 1112.2 and 1234.5 keV γ rays at the top of the band could not be attempted due to a lack of adequate statistics in the data. Tentative spins of $(37/2^+)$ and $(39/2^+)$ are nevertheless suggested for the two highest-energy states at 7510.3 and 7764.9 keV, respectively, based on the systematics within the band.

C. Band 3

As noted earlier in this text, the present work attempts a study of only one of three previously reported decoupled

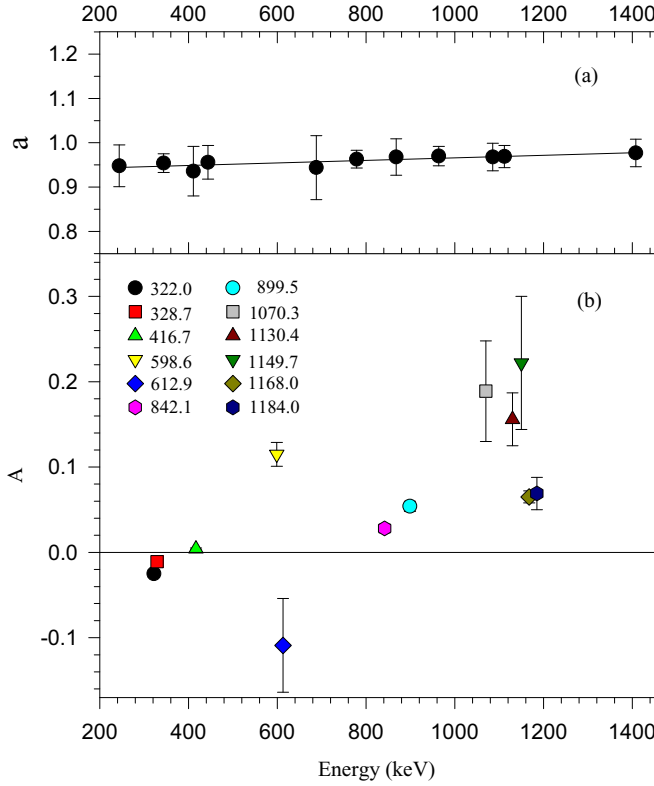


FIG. 5. Plots of (a) the normalization factor a in the polarization measurements and (b) the experimental polarization asymmetry A (defined in the text) as a function of γ -ray energy.

intruder bands in ^{113}Sn [8]. This is labeled band 3 in Fig. 1. Low-lying states of the other two intruder bands, marked band 1 and band 2 in Ref. [8], were shown to decay weakly into the states of band 3. Some of these linking transitions with energies 739, 820, 851, and 961 keV (γ -ray energies as in Fig. 1 in Ref. [8]) were also observed in the present work. However, their intensities were too weak to have an effect on the analyses of the data related to band 3 in the present work.

Band 3 is a negative-parity sequence of states built upon the $23/2^-$, 3901.2 keV level. The band has been previously reported only by Sears *et al.* [8]. Although the band was observed up to a spin of $(63/2^-)$ in Ref. [8], states only up to $51/2^-$ could be confirmed in the present work. The sum of the spectra gated on the 810.2, 811.6, and 930.2 keV transitions, presented

in Fig. 3(e), shows the γ rays belonging to band 3 that have been observed in the present work. Only the 90° projection is included in this spectrum. The bandhead at 3901.2 keV decays to the 1907.0 keV state along two paths, one of which is about twice as strong as the other (see Fig. 1 and Table I).

Reliable DCO measurements were possible for transitions depopulating states up to $43/2^-$. The R_{DCO} values for these transitions (Table 1) are consistent with their stretched-quadrupole nature and confirm the earlier spin assignments [8] for the states. Although measurements were not possible for the 1125.2 and 1306 keV γ rays from the 9934.9 and 11240.8 keV states, respectively, firm spins assignments are indicated in Fig. 1 for all states observed in band 3, based on earlier work [8].

Lifetimes have been determined for the first time for six states up to spin $47/2^-$ in band 3, with the last one being an upper limit. The results are summarized in Table II. Gated Doppler-shifted lineshape spectra at 148° and the corresponding unshifted spectra at 90° with respect to the beam direction are shown in Fig. 4 for the 930.2, 1026.9, and 1037.1 keV transitions. The theoretical fits to the observed spectra, obtained using LINESHAPE [12], are included in the figure. Analyses of the lineshapes, especially for the overlapping 1026.9 and 1037.1 keV transitions, are discussed below.

The fitting of the experimental spectra with the theoretical lineshapes was started with the highest observed transition in the band with reasonable statistics, in this case the 1125.2 keV transition depopulating the 9934.9 keV state. Considering the large uncertainty in the feeding-time information for this state (since the lifetime of the next-higher-energy state is not known), LINESHAPE provides only an effective lifetime (stated as the upper limit) of $\tau \leq 0.12$ ps for the 9934.9 keV state. This lifetime information, along with the respective side-feeding-time data (provided as an input parameter to the LINESHAPE code; see discussion below), were then used as parameters in the code for the estimation of the lifetime of the 8809.7 keV state depopulating by the 1026.9 keV transition. The plots of the experimental spectrum and the theoretical fits to the observed lineshape are shown in Fig. 4(b). As can be seen from the figure, the Doppler-shifted component of the 1037.1 keV transition interferes strongly with the lineshape of the 1026.9 keV transition at 148° to the beam. This has necessitated a detailed procedure for the analysis of the lineshape for these two transitions. Initially, an assumed shifted component of the 1037.1 keV transition is used to

TABLE II. Present experimental results on mean lifetime (τ), $B(E2)$ rates, transition quadrupole moments (Q_t), and quadrupole deformation (β_2) for band 3 in ^{113}Sn .

E_x (keV)	E_γ (keV)	Spin $J_i^\pi \rightarrow J_f^\pi$	τ (ps)	$B(E2)$ (W.u.)	Q_t (eb)	β_2^a
4712.8	811.6	$27/2^- \rightarrow 23/2^-$	$0.50^{+0.04}_{-0.03}$	$143.0^{+8.0}_{-10.5}$	$3.94^{+0.11}_{-0.15}$	0.27 ± 0.01
5643.0	930.2	$31/2^- \rightarrow 27/2^-$	$0.33^{+0.07}_{-0.05}$	$110.2^{+21.8}_{-19.9}$	3.38 ± 0.32	0.24 ± 0.02
6680.1	1037.1	$35/2^- \rightarrow 31/2^-$	$0.22^{+0.06}_{-0.05}$	$95.4^{+27.1}_{-20.8}$	$3.09^{+0.41}_{-0.36}$	$0.22^{+0.03}_{-0.02}$
7782.8	1102.7	$39/2^- \rightarrow 35/2^-$	$0.26^{+0.05}_{-0.04}$	$58.6^{+8.9}_{-8.6}$	2.39 ± 0.18	0.17 ± 0.01
8809.7	1026.9	$43/2^- \rightarrow 39/2^-$	0.32 ± 0.04	$68.7^{+8.6}_{-8.1}$	2.56 ± 0.16	0.18 ± 0.01
9934.9	1125.2	$47/2^- \rightarrow 43/2^-$	≤ 0.12	≥ 118	≥ 3.3	

^aCalculated assuming $\gamma = 0^\circ$.

obtain an approximate lifetime for the 8809.7 keV level from the lineshape in Fig. 4(b). This result is used to derive, once again approximately, the lifetime of the 7782.8 keV state (Fig. 1) from an analysis of the lineshape of the 1102.7 keV transition (not shown in Fig. 4). The lifetimes of the 8809.7 and 7782.8 keV states, so derived, are then used to calculate the shifted component of the 1037.1 keV transition, depopulating the 6680.1 keV level. A feedback of this Doppler-shifted component of the 1037.1 keV transition into the lineshape for the 1026.9 keV transition then leads to more realistic lifetime results for the 8809.7 and 7782.8 keV levels. The process is repeated a few times before the final results are obtained for the 8809.7, 7782.8, and 6680.1 keV states. Analysis of the lineshapes for the 811.6 and 930.2 keV γ rays from the 4712.8 and 5643.0 keV levels, respectively, were straightforward.

The level lifetimes were corrected for both discrete feedings from the higher-energy states and direct- or side-feedings from the continuum. The side-feeding times for the states of band 3 in ^{113}Sn were constrained to be similar to those used for ^{113}Sb [6], populated in the same experiment. The side-feeding time was therefore assumed to be 0.1 ps for the highest observed state in the band (in this case the 11240.8 keV state; see Fig. 1) and increase progressively by 0.05 ps per MeV decrease of excitation energy. The reliability of this method of estimation of the side-feeding times is supported by the fact that the average transition quadrupole moment for the intruder rotational band in ^{113}Sb , reported earlier by Janzen *et al.* [2], was successfully reproduced in Ref. [6]. The side-feeding time was calculated for each state following this procedure and provided as an input parameter in the LINESHAPE code. The code then used this data and the discrete feeding-time information for each state (already obtained from the preceding fits; discussed above) for calculating the fits to the observed spectra for successive lower-lying transitions in the band, selected one at a time. The errors stated in the level lifetimes τ and the transition quadrupole moments Q_i in Table II include the statistical uncertainties in the data and the effects of a 30% uncertainty in the side-feeding times. Experimentally measured side-feeding times for two states in ^{112}Sn (see Table 2 in Ref. [5]) have a similar error of about 30%. Additional uncertainties of up to 15% inherent in the electronic stopping powers used in LINESHAPE are not included in the results.

IV. DISCUSSION

Nuclei near the closed proton shell at $Z = 50$ are known to possess a wealth of both collective and noncollective structures. The low-spin states in ^{113}Sn are mainly spherical and vibrational in nature that arise from the coupling of neutrons in the $g_{7/2}$, $d_{5/2}$, and $h_{11/2}$ orbitals, which lie near the Fermi surface, to the low-energy spherical and vibrational states in the neighboring ^{112}Sn .

Band 2 is a new $\Delta I = 1$, positive-parity sequence of eight states built upon the $25/2^+$, 4055.8 keV level (Fig. 1). The band extends up to an excitation energy of 7764.9 keV and spin ($39/2^+$). Given that a positive parity is unambiguously assigned to band 2 (see Sec. III B), it is plausible to argue that the band is based upon a deformed 2p-2h proton configuration coupled to the odd valence neutron occupying positive-parity orbitals such as $g_{7/2}$ or $d_{5/2}$. The positive parity of the states

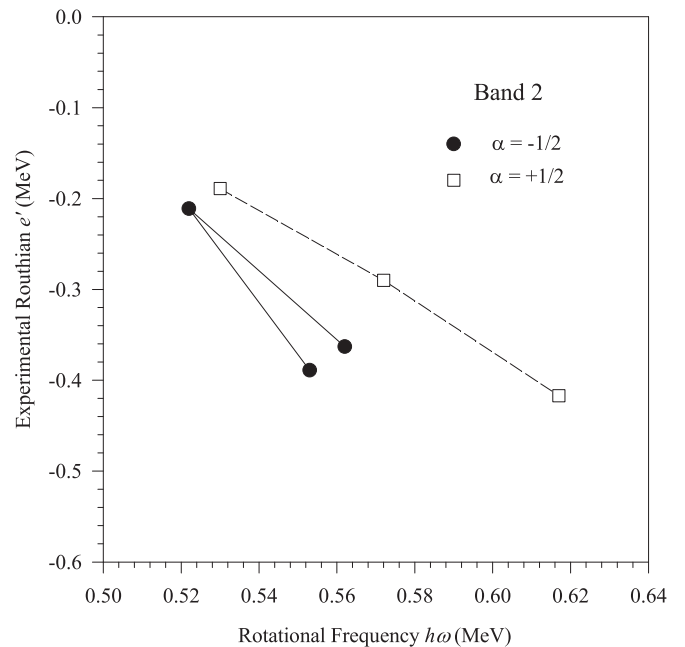


FIG. 6. Experimental Routhians e' for the $\alpha = -1/2$ (favored) and the $\alpha = +1/2$ (unfavored) signature partners of band 2.

also imply that there are an even number of neutrons in the $h_{11/2}$ orbital with the remaining neutrons outside the ^{100}Sn core distributed in the $g_{7/2}$, $d_{5/2}$ (nearly degenerate) and $s_{1/2}$ orbitals.

Both the favored ($\alpha = -1/2$) and unfavored ($\alpha = +1/2$) signature partners of band 2 are observed (Fig. 1) in the present work. Unlike strongly coupled bands, the states belonging to band 2 show a significant amount of signature splitting and could therefore be interpreted as a decoupled structure. The weak intensity of the $\Delta I = 1$ transitions relative to the $E2$ transitions (Table I) is consistent with the decoupled nature of the band. The experimental quasiparticle Routhians for the two signature bands, shown in Fig. 6, indicate a signature splitting of $\Delta e' \approx 100$ keV at $h\omega = 0.56$ MeV. The Harris parameters used to describe the energy of the core are $J_0 = 15\hbar^2/\text{MeV}$ and $J_1 = 25\hbar^4/\text{MeV}^3$ [16]. The signature splitting for band 2 is, however, relatively less compared to decoupled bands such as band 3 where the odd neutron occupies the lower-energy states (with $\Omega = 1/2$ and $3/2$) of the high- j $h_{11/2}$ subshell leading to a large signature splitting. The unfavored signature partner for band 3 is therefore pushed up substantially in energy far above the yrast line and is not observed experimentally. The relatively smaller signature splitting for band 2 suggests that the odd valence neutron could be occupying the lower midshell part of the $g_{7/2}$ or $d_{5/2}$ subshells. Considering that ^{113}Sn has thirteen neutrons outside the ^{100}Sn core, it is plausible to argue that four neutrons would occupy the $h_{11/2}$ orbital in order that the last odd neutron can occupy a relatively low- Ω (such as $\Omega = 3/2, 5/2$) state of the $g_{7/2}$ or the $d_{5/2}$ orbital.

It may be noted in this context that the $[21,4]$ negative-parity band in ^{113}Sb also has four neutrons in the $h_{11/2}$ orbital but the unfavored band is not observed (signature splitting is large) due to the presence of the odd-proton in the $\Omega = 1/2$ state of the $h_{11/2}$ orbital. However, the negative-parity $\Delta I = 2$ band in ^{115}Sn has been reported to show both the

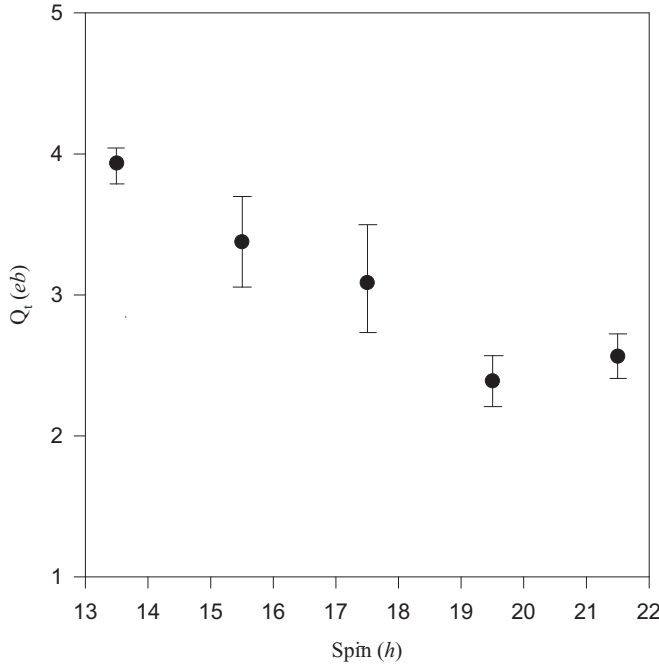


FIG. 7. Plot of transition quadrupole moments Q_t for band 3 as a function of spin I .

signature partners [16] with a signature splitting of about 150–300 keV in the frequency range 0.3–0.5 MeV. A difference of this band in ^{115}Sn with the [20,3] band in ^{113}Sn in terms of their signature splittings probably lies in the fact that the two extra neutrons in ^{115}Sn could be occupying the $h_{11/2}$ orbital with the last odd neutron lying in the midshell of the $h_{11/2}$ orbital. A similar situation possibly exists for the positive-parity band 2 in ^{113}Sn where the last odd-neutron may be occupying a lower midshell orbital in the $g_{7/2}$ or the $d_{5/2}$ subshells leading to similar degrees of signature splittings. Based on these and other arguments presented in the two preceding paragraphs, the [20,4] configuration may be tentatively assigned to band 2 in ^{113}Sn . The [20,4] configuration has been previously predicted to be energetically favored at spins less than about $25\hbar$ [8].

Band 3 is interpreted as a deformed intruder band resulting from the coupling of the $\nu h_{11/2}$ orbital with the deformed proton 2p-2h state $\pi[(g_{7/2})^2(g_{9/2})^{-2}]$. Lifetime measurements for five states with excitation energies $E_x \leq 8809.7$ keV ($I^\pi \leq 43/2^-$) in the present work suggest a significant collectivity for the lower-spin states in the band. The reduced transition probability for the 811.6 keV transition depopulating the $27/2^-$, 4712.8 keV state near the bandhead, for example, is $B(E2) = 143.0^{+8.0}_{-10.5}$ W.u. (Table II). Thereafter, the $B(E2)$ rates decrease steadily to less than half this value for the $39/2^-$ and $43/2^-$ states. These measurements also lead to an average quadrupole deformation of $\beta_2 = 0.22 \pm 0.02$ for states up to $43/2^-$, assuming axial symmetry. A similar average deformation of $\beta_2 = 0.24 \pm 0.02$ was previously obtained for the lower energy states in the $\nu h_{11/2}$ intruder band in ^{111}Sn by the present authors [4]. Indeed, the negative-parity rotational bands in ^{109}Sn [17], ^{111}Sn [1,4], and ^{113}Sn [8] have a similarity in their structures, and the high-spin members of these bands have been understood to arise from the configuration [20,3] $^-$

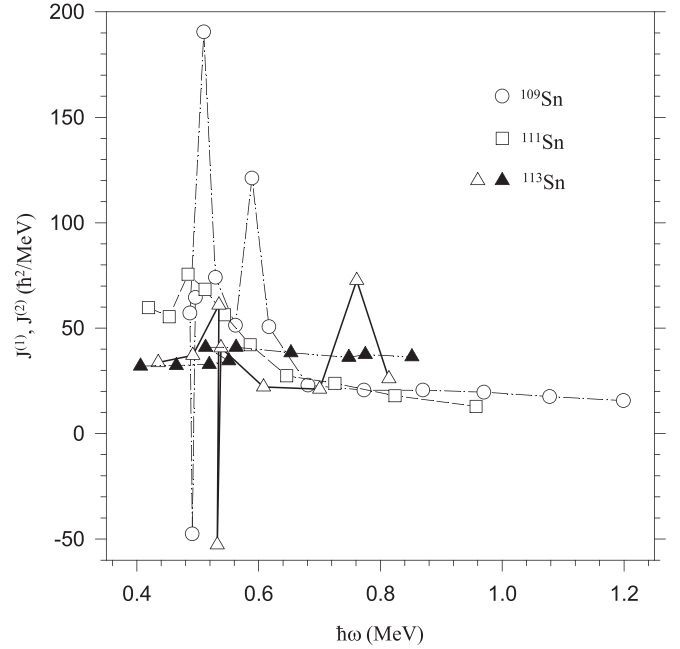


FIG. 8. Plots of dynamic moments of inertia $J^{(2)}$ for ^{109}Sn [17] (open circles), ^{111}Sn [1] (open squares), and ^{113}Sn (from present work and Ref. [8]) (open triangles) for bands with the configuration [20,3] (see text). Plot of the kinematic moment of inertia $J^{(1)}$ for the [20,3] band in ^{113}Sn is also shown using filled triangles.

where the $-1/2$ signature band is lower in energy and is hence the favored signature partner.

As noted in the introduction, many of these intruder bands, observed in the $Z = 50$ nuclei, have displayed the effect of gradually decreasing dynamic moment of inertia to a value which is about a third of the rigid-body value and have been explained as smoothly terminating bands. The nuclear shape makes a transition from collective prolate at low spins to noncollective oblate near the terminating states. The decrease in collectivity with increasing spin is manifested in the values of the reduced transition probabilities $B(E2)$ and the transition quadrupole moments Q_t , derived from a measurement of the level lifetimes. The transition quadrupole moments for band 3 in ^{113}Sn , plotted as a function of level spin in Fig. 7, shows an overall decreasing trend in spite of the somewhat large experimental errors in some of the Q_t values. This suggests that band 3 could indeed be identified as a possible candidate for a terminating band. The decrease in the value of Q_t at spin $39/2^-$ followed by a small increase for the $43/2^-$ state is possibly due to the alignment of the second pair of $h_{11/2}$ neutrons (alignment of the first pair is Pauli blocked) at a rotational frequency of $\hbar\omega \sim 0.53$ MeV (see Fig. 8). The [20,3] bands in both the neighboring Sn isotopes; namely, $^{111,115}\text{Sn}$, are previously reported to exhibit this alignment at a similar frequency [1,18]. However, a more clear insight into the behavior of the Q_t values with spin and hence the structure of the band at high spins could be obtained if the lifetime measurements could be extended to states closer to termination.

The dynamic moment of inertia $J^{(2)}$ for the [20,3] $^-$ band in ^{113}Sn has been plotted as a function of rotational frequency $\hbar\omega$

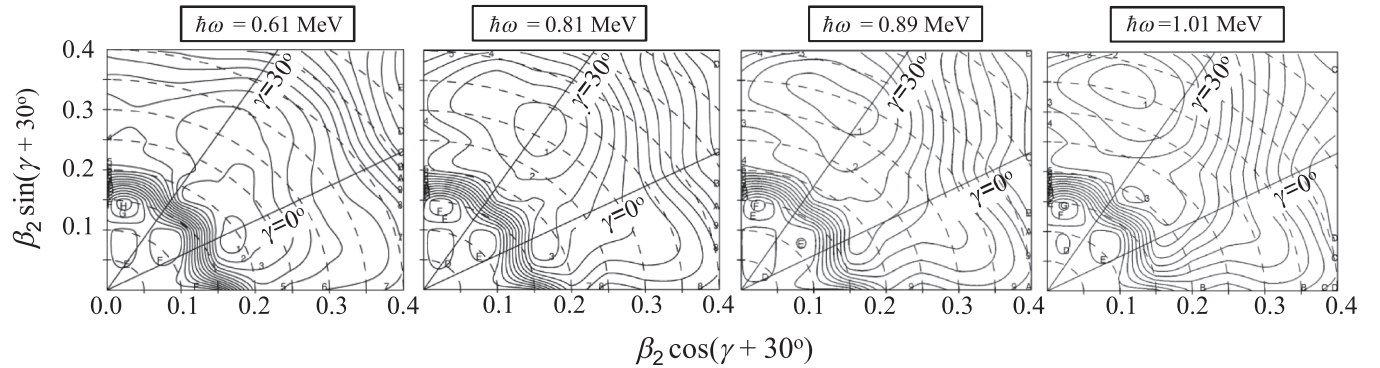


FIG. 9. Total-Routhian-surface plots for band 3 in the β_2 - γ plane for four rotational frequencies as indicated.

in Fig. 8. The $J^{(2)}$ plots for similar $[20,3]^-$ bands in $^{109,111}\text{Sn}$, previously interpreted as smoothly terminating bands, are also shown in the same figure for comparison. The data for the $J^{(2)}$ plot for ^{109}Sn are taken from Ref. [17] and includes all data points from spin $19/2^-$ onwards, although only states above spin ($51/2^-$) are interpreted as belonging to the $[20,3]$ configuration. The data for the $J^{(2)}$ plot for ^{111}Sn are from Ref. [1]. As expected, the plots show that, for both ^{109}Sn and ^{111}Sn , the $J^{(2)}$ values fall off to about $15\hbar^2/\text{MeV}$ for states near termination, which is less than half of the rigid-body value. For ^{113}Sn , both the present data as well as those reported by Sears *et al.* [8] (the last three data points in the plot for ^{113}Sn are from Ref. [8]) have been included in Fig. 8. Although the last band crossing occurs at a different frequency in ^{113}Sn relative to the other two Sn isotopes (explained in Ref. [8]), the $J^{(2)}$ value falls off to $26\hbar^2/\text{MeV}$ at $\hbar\omega = 0.81$ MeV ($I^\pi = 59/2^-$) in ^{113}Sn . It may be noted that, while states only up to $(63/2^-)$ are known [8], the $[20,3]$ configuration [i.e., $\pi[(g_{9/2})^{-2}(g_{7/2}, d_{5/2}^2)] \otimes \nu[(h_{11/2})^3(g_{7/2}, d_{5/2})^{10}]$ relative to the $Z = N = 50$ doubly closed shell] in ^{113}Sn is expected to terminate at a somewhat higher spin of $75/2^-$. With further alignment of particles unlikely at frequencies greater than $\hbar\omega = 0.81$ MeV, the three unobserved higher-energy states above spin $(63/2)^-$, until the terminating state at $75/2^-$, are expected to be built at larger energy costs, leading to smaller values of dynamic moments of inertia. This would bring the $J^{(2)}$ values for ^{113}Sn into closer agreement with those in $^{109,111}\text{Sn}$. Furthermore, the kinematic moment of inertia $J^{(1)}$ for band 3 in ^{113}Sn , plotted using filled triangles in Fig. 8, are significantly larger than the $J^{(2)}$ values at high spins. This behavior of the dynamic as well as of the kinematic moments of inertia for band 3 therefore might appear to be consistent with the nature of smoothly terminating bands. However, the states above spin $(63/2)^-$ have not been observed so far and only the actual behavior of $J^{(2)}$ in this region of rotational frequencies can confirm if the band terminates smoothly. A possible interaction of the states of band 3 with other configurations may cause the dynamic moment of inertia to become an irregular function of rotational frequencies. Indeed, the energies of the $55/2^-$ states in band 3 and another decoupled band (labeled band 2 in Ref. [8]; not shown in the present work) differ only by about 110 keV and the possibility of an interaction between the two bands cannot be excluded [8].

The total-Routhian-surface (TRS) calculations using a deformed Woods–Saxon potential and monopole pairing have been performed for band 3 in ^{113}Sn . The calculations were carried out for the $[20,3]$ configuration and the total energy was minimized in the (β_2, γ) space with respect to the hexadecapole deformation β_4 . The results from the calculations at the four rotational frequencies $\hbar\omega = 0.61, 0.81, 0.89,$ and 1.01 MeV are shown in Fig. 9. The calculated deformation parameters $(\beta_2, \gamma) = (0.19, -3.30^\circ)$ at $\hbar\omega = 0.61$ MeV ($I^\pi \simeq 47/2^-$) are in good agreement with the experimental value of $\beta_2 = 0.18 \pm 0.01$ for the $43/2^-$ state (Table II). The TRS plots also show that the nuclear shape evolves from collective prolate at $\hbar\omega = 0.61$ MeV to a triaxial shape at 0.81 MeV before assuming a γ -soft triaxial shape at 0.89 MeV that appears to be approaching a noncollective oblate shape. Calculations at the expected terminating frequency of 1.01 MeV indicates that the shape tends to become less γ soft and more oblate. Although such indications suggest that band 3 evolves from significant collectivity at low spin to a particle-hole noncollective terminating state at high spin, a clear insight into the nature of the termination, smooth or unsmooth, can only be obtained if the band could be observed up to higher spins.

V. CONCLUSION

Structure of rotational bands in ^{113}Sn have been investigated in the present work by using the reaction $^{100}\text{Mo}(^{19}\text{F}, p5n)$ at a projectile energy of 105 MeV. A new decoupled band built on the $25/2^+$, 4055.8 keV state and extending up to 7764.9 keV and spin $(39/2^+)$ has been identified. The assignment of a positive parity and a significant amount of signature splitting ($\Delta e' \approx 100$ keV at $\hbar\omega = 0.56$ MeV) between the favored $\alpha = -1/2$ and the unfavored $\alpha = +1/2$ signature partners favors the interpretation of the states as arising from a deformed 2p-2h proton configuration coupled to an odd valence neutron in the lower midshell ($\Omega = 3/2, 5/2$) part of the $d_{5/2}$ or the $g_{7/2}$ orbital. Arguments are proposed to suggest that the $[20,4]$ configuration may be tentatively assigned to band 2. Lifetimes of six states up to 9934.9 keV, including an upper limit for the last state, have been measured from DSA data for the first time. The measurements indicate an average quadrupole deformation $\beta_2 = 0.22 \pm 0.02$ for the five states up to 8809.7 keV. The transition quadrupole moments show a gradual decrease with spin suggesting a reduction

in collectivity. It is likely that an interaction of band 3 at a spin of $55/2^-$ with other configurations may contribute to the $J^{(2)}$ values to behave irregularly as a function of rotational frequency at large spins.

ACKNOWLEDGMENTS

The first author (P.B.) gratefully acknowledges the financial support provided by the Council of Scientific and Industrial

Research (CSIR), Human Resource Development Group, vide Project No. 21(0943)/12/EMR-II for the Emeritus Scientist scheme. The authors thank the Indian National Gamma Array collaboration for help in setting up the array. The assistance provided by the Pelletron operating staff is acknowledged. Thanks are also due to Mr. Ajoy Mitra of the Saha Institute of Nuclear Physics, Kolkata for help during the experiment and to Mr. Iqbal of the Variable Energy Cyclotron Centre, Kolkata for preparing the targets.

-
- [1] D. R. LaFosse, D. B. Fossan, J. R. Hughes, Y. Liang, P. Vaska, M. P. Waring, J.-y. Zhang, R. M. Clark, R. Wadsworth, S. A. Forbes, and E. S. Paul, *Phys. Rev. C* **51**, R2876 (1995).
- [2] V. P. Janzen, H. R. Andrews, B. Haas, D. C. Radford, D. Ward, A. Omar, D. Prévost, M. Sawicki, P. Unrau, J. C. Waddington, T. E. Drake, A. Galindo-Uribarri, and R. Wyss, *Phys. Rev. Lett.* **70**, 1065 (1993).
- [3] P. Banerjee, S. Ganguly, M. K. Pradhan, H. P. Sharma, S. Muralithar, R. P. Singh, and R. K. Bhowmik, *Phys. Rev. C* **83**, 024316 (2011).
- [4] S. Ganguly, P. Banerjee, I. Ray, R. Kshetri, R. Raut, S. Bhattacharya, M. Saha-Sarkar, A. Goswami, and S. K. Basu, *Phys. Rev. C* **78**, 037301 (2008).
- [5] S. Ganguly, P. Banerjee, I. Ray, R. Kshetri, R. Raut, S. Bhattacharya, M. Saha-Sarkar, A. Goswami, S. Mukhopadhyay, A. Mukherjee, G. Mukherjee, and S. K. Basu, *Nucl. Phys. A* **789**, 1 (2007).
- [6] P. Banerjee, S. Ganguly, M. K. Pradhan, H. P. Sharma, S. Muralithar, R. P. Singh, and R. K. Bhowmik, *Phys. Rev. C* **87**, 034321 (2013).
- [7] R. Wadsworth, R. M. Clark, J. A. Cameron, D. B. Fossan, I. M. Hibbert, V. P. Janzen, R. Krücken, G. J. Lane, I. Y. Lee, A. O. Macchiavelli, C. M. Parry, J. M. Sears, J. F. Smith, A. V. Afanasjev, and I. Ragnarsson, *Phys. Rev. Lett.* **80**, 1174 (1998).
- [8] J. M. Sears, S. E. Gundel, D. B. Fossan, D. R. LaFosse, P. Vaska, J. DeGraaf, T. E. Drake, V. P. Janzen, D. C. Radford, Ch. Droste, T. Morek, U. Garg, K. Lamkin, S. Naguleswaran, G. Smith, J. C. Walpe, R. Kaczarowski, A. V. Afanasjev, and I. Ragnarsson, *Phys. Rev. C* **58**, 1430 (1998).
- [9] A. V. Afanasjev and I. Ragnarsson, *Nucl. Phys. A* **591**, 387 (1995).
- [10] I. Thorslund, D. B. Fossan, D. R. LaFosse, H. Schnare, K. Hauschild, I. M. Hibbert, S. M. Mullins, E. S. Paul, I. Ragnarsson, J. M. Sears, P. Vaska, and R. Wadsworth, *Phys. Rev. C* **52**, R2839 (1995).
- [11] R. K. Bhowmik, INGASORT Manual (private communication).
- [12] J. C. Wells and N. R. Johnson, LINESHAPE: A Computer Program for Doppler-Broadened Lineshape Analysis, ORNL Physics Division Progress Report No. ORNL-6689 (1991).
- [13] E. S. Macias *et al.*, *Comput. Phys. Commun.* **11**, 75 (1976).
- [14] Jean Blachot, *Nucl. Data Sheets* **111**, 1471 (2010).
- [15] L. Käubler, Yu. N. Lobach, V. V. Trishin, A. A. Pasternak, M. F. Kudojarov, H. Prade, J. Reif, R. Schwengner, G. Winter, J. Blomqvist, and J. Döring, *Z. Phys. A: Hadrons Nucl.* **358**, 303 (1997).
- [16] A. Savelius, S. Juutinen, K. Helariutta, P. Jones, R. Julin, P. Jämsen, M. Muikku, M. Piiparinen, J. Suhonen, S. Törmänen, R. Wyss, P. T. Greenlees, P. Simecek, and D. Cutoiu, *Nucl. Phys. A* **637**, 491 (1998).
- [17] L. Käubler, H. Schnare, D. B. Fossan, A. V. Afanasjev, W. Andrejtscheff, R. G. Allat, J. de Graaf, H. Grawe, I. M. Hibbert, I. Y. Lee, A. D. Macchiavelli, N. O'Brien, K.-H. Maier, E. S. Paul, H. Prade, I. Ragnarsson, J. Reif, R. Schubart, R. Schwengner, I. Thorslund, P. Vaska, R. Wadsworth, and G. Winter, *Z. Phys. A: Hadrons Nucl.* **356**, 235 (1996).
- [18] J. M. Sears, D. B. Fossan, S. E. Gundel, I. Thorslund, P. Vaska, and K. Starosta, *Phys. Rev. C* **55**, 1096 (1997).